Quantifying Emergent Fluid Dynamics Using Reynolds-Interpolated Fluid Reduced-Order Models

Chris Edwards*
North Carolina State University, Raleigh, NC 27695

Michael W. Lee†
NASA Langley Research Center, Hampton, VA 23681

Donya Ramezanian‡
University of Southern California, Los Angeles, CA 90089

Ralph C. Smith§
North Carolina State University, Raleigh, NC 27695

Fluid reduced-order models (ROMs) that qualify the flow physics within the problem's physical domain are usually constrained in accuracy to only the parameter points; e.g., Reynolds and Mach numbers, at which reference data were provided. Interpolation-focused quantity-of-interest ROMs are often structured differently and fail to provide flow volume data with the same quality – if at all. In this paper, techniques that reside at the intersection of these two ROM schools – flow physics ROMs that can be interpolated within a parameter space of interest – are explored. Using a combination of existing and novel techniques, emergent physics are identified using a fluid ROM at parameter points that are not provided in the ROM training data.

Nomenclature

a	=	modal coefficient
C	=	reduced-order model constant vector
G	=	Grassman manifold
L	=	reduced-order model linear matrix
M	=	reduced-order model mass matrix
p	=	fluid static pressure
P	=	reduced-order model pressure matrix
Q	=	reduced-order model nonlinear matrix
r	=	dimension of POD subspace
Re	=	Reynolds number
s	=	new parameter point for interpolation
t	=	time
u	=	fluid velocity vector
U	=	left singular vector matrix
V	=	right singular vector matrix
$\mathbf{x}$	=	spatial position vector
Γ	=	spatial domain boundary
ϕ	=	spatial mode
Φ	=	modal basis
Σ	=	diagonal singular value matrix
Ω	=	spatial domain

*Doctoral Candidate, Department of Mathematics, North Carolina State University.
†Research Aerospace Engineer, Configuration Aerodynamics Branch, NASA Langley Research Center, AIAA Member.
‡Postdoctoral Scholar, Viterbi School of Engineering, University of Southern California.
§Distinguished University Professor, Department of Mathematics, North Carolina State University.

EDL	=	Entry, Descent and Landing
MCMC	=	Markov Chain Monte Carlo
MLUQ	=	Machine Learning with Embedded Uncertainty Quantification
ODE	=	Ordinary Differential Equation
POD	=	Proper Orthogonal Decomposition
ROM	=	Reduced-order Model

I. Background and Motivation

Vehicles designed for planetary entry, descent, and landing (EDL) experience a gamut of extreme environments. Within this broad parameter space, the vehicle must perform within very tight trajectory tolerances in order for its landing to be as precise as possible and its cargo to remain safe. As lander geometries become more complicated and deviate further from existing, trusted flight envelopes, e.g., those of the Viking program, more rigorous uncertainty quantification becomes a necessary part of the design process. This is a focus of the Mars Lander Aerodynamic Model Data Fusion using Machine Learning with Embedded Uncertainty Quantification (AeroFusion-MLUQ) initiative recently undertaken by researchers at the NASA Langley Research Center and collaborating universities [1].

Uncertainty quantification can be performed for aerodynamic models through Bayesian Markov chain Monte Carlo (MCMC) techniques. However, these techniques typically require numerous model evaluations, e.g., on the order of $O(10^4)$. This in turn necessitates the use of fast and accurate flow solvers, which exhibit sensitivity to flow parameters and simulation hyperparameters similar to the higher-cost, higher-fidelity flow solvers used to generate the original design cycle data. Fluid reduced-order models (ROMs), with explicit dependence on parameters like Reynolds number, are one such tool. In this work, we focus on ROMs that are parametrically sensitive but do not require modal matrix operations to be performed during the model evaluation itself. While this limits the complexity of the models that can be implemented, it keeps the ROM's computational cost low enough that MCMC efforts can yield meaningful results without intractable computation times.

Often for design optimization or uncertainty quantification, high fidelity computational fluid dynamics (CFD) simulations must be performed at a large number of points within a parameter space. However, since these CFD simulations are computationally expensive, computing data at a high density within the parameter space presents a significant challenge. To address the large computational cost of high fidelity CFD models, reduced-order modeling techniques are commonly employed to obtain low-dimensional models for the simulation of fluid flows [2, 3]. These ROMs, often based on the proper orthogonal decomposition (POD) and Galerkin projection, are able to achieve reasonable accuracy at a much cheaper computational cost [4]. The accuracy of such reduced-order models for fluid flows is typically constrained to parameter points for which reference data are provided. Therefore, techniques have been developed for constructing accurate fluid flow reduced-order models at parameter points where no reference data are available [5–7].

Application of ROMs for the purpose of parameter interpolation has been explored more thoroughly in the context of quantities of interest (QoI). Rather than simulate the entire fluid flow with a ROM and then extract QoIs, like the lift and drag coefficients, the system of QoIs can themselves be modeled, for example as a linear time-invariant system [8] or as a constrained dynamical system [9]. However, these models are far more likely to miss emergent physics in the underlying systems because they do not model it directly. This motivates yet other methods, which are specifically designed to qualify bifurcations within dynamical systems [10], though these too are limited in their generalizability.

More general parametrized fluid reduced-order models, which are capable of accurate simulations at parameter points not included in the training data, are the focus of this research. Existing techniques in this category include utilizing a single global basis, interpolating local bases, interpolating local reduced-order system matrices, and interpolating local reduced-order transfer functions [5]. Global basis techniques include basis concatenation of precomputed bases and the spanning ROM approach, which forms a global basis by performing POD on a collection of snapshots from a number of parameter points [6]. Basis concatenation offers a simple approach for the construction of a global basis to be utilized for parametric ROM construction and is useful for MCMC considerations since the ROM system matrices do not need to be recomputed for new points in the parameter space. The spanning ROM approach introduced in Ref. [6] also does not require recomputation of the ROM system matrices via Galerkin projection and instead utilizes interpolation of the ROM system matrices when the ROM system matrices depend on the parameter/parameters. Typically in basis interpolation, two precomputed orthonormal bases associated with given parameters are interpolated within a tangent space to a Grassman manifold, to which the subspace spanned by each of the bases is an element [11]. The need to recompute the ROM system matrices for new parameters generally precludes this method from MCMC techniques for this problem due to the computational cost of constructing the ROM matrices, however, we include this technique for accuracy comparisons to other techniques since this method has been successfully utilized for the adaptation of aeroelastic ROMs [7].

In this paper, we investigate the construction and performance of parametric reduced-order models based directly on the incompressible Navier-Stokes equations. Using regularized lid-driven cavity data [12] as the test case, we will show that emergent physics in the form of unique frequency-domain responses can be found at parameter points not provided for the ROM's training. We employ global basis and basis interpolation techniques to construct parametric ROMs parametrized by Reynolds number. The performance and robustness of the techniques are assessed by comparing two QoIs obtained from both the ROM and from reference direct numerical simulation (DNS) data: the global kinetic energy and the global enstrophy. We investigate three specific methods for constructing parametric reduced-order models: formulating a global basis using the spanning ROM approach [6], implementing a simple basis concatenation technique, and interpolating bases using the Reynolds number as the reference point for interpolation.

II. Methodology

A. Parametric ROM Construction

We consider three methods for construction of parametric reduced-order models: the spanning ROM method, basis interpolation and basis concatenation. In the spanning ROM method, data snapshots corresponding to different parameter points across the parameter space are used to form a snapshot matrix. Proper orthogonal decomposition is performed on this collection of snapshots and the obtained spanning basis is used to form the ROM system matrices, via Galerkin projection, for each parameter value used to form the collection of snapshots. If the ROM matrices do not depend on the parameters, then the ROM system matrices will be the same for each parameter value since the same basis is used for each computation. To compute the reduced-order model for a new parameter value not in the set used to form the spanning ROM basis, elementwise cubic spline interpolation is performed among the known ROM matrices [6]. This interpolation may be performed either in the original coordinate space or a tangent space of a manifold where the variation of the elements of the ROM matrices as a function of the parameter is smooth. We note that a downside of this approach is the computational cost of performing POD on the collection of snapshots.

In the univariate basis interpolation method, two precomputed orthonormal bases, represented by modal matrices Φ_0 and Φ_1, are interpolated following the techniques introduced for univariate parameter interpolation of bases in Ref. [7] with a small adaptation to the formulation. The two bases, Φ_0 and Φ_1, span r^0 and r^1 dimensional subspaces of $\mathbb{R}^n$. These subspaces are elements of the Grassman manifolds (G_{n,r^0} for the subspace spanned by Φ_0 and G_{n,r^1} for the subspace spanned by Φ_1). The Grassman manifold $G_{n,r}$ is the set of all r dimensional subspaces of $\mathbb{R}^n$.

We summarize the interpolation procedure in Algorithm 1. We adapt the original formula by replacing the inverse with the pseudo-inverse to permit bases of different sizes in terms of number of modes, r^0 and r^1. We note that whereas this method provides a parameter-dependent basis, the ROM matrices must be recomputed every time we construct a new basis via this method, preventing this method's use for MCMC methods since construction of the ROM matrices for the incompressible ROM is not computationally cheap.

The general basis interpolation formula detailed in Ref. [7] extends the univariate formula to an arbitrary number of bases and physical or modeling parameters. We summarize this procedure in Algorithm 2. Each basis spans a subspace $\{S_i\}_{i=0}^n$. A subspace is chosen as a reference point for the interpolation, and the other subspaces are mapped to a matrix Σ_i representing a point on the tangent space, T_0, using the logarithm map. Next, each entry of the matrix $\Gamma(s)$ for the new parameter value s is computed by interpolating the entries of the matrices $\{\Sigma_i\}_{i=1}^n$. Finally, $\Phi(s)$ is obtained from $\Sigma(s)$ through the exponential map.

In the concatenated basis approach, precomputed bases corresponding to given parameter values are concatenated together to form a new basis, which is used to construct ROMs for parameter values ranging across the parameter values of the bases used to construct the new concatenated basis. Consider k bases corresponding to k parameter values or k parameter configurations within a parameter space. We construct a new basis for parametric ROM construction by concatenating the k bases. This concatenated basis is utilized via Galerkin projection to construct a parametric reduced-order model capable of accurate interpolation at new parameter values or configurations within the parameter space.

In Section II.B, we introduce the incompressible Navier-Stokes equations and and the set of coupled ODEs that we solve with the parametric ROM techniques.

Algorithm 1 Univariate Basis Interpolation

Input: 2 orthonormal bases (Φ_0, Φ_1) with associated parameters (s_0, s_1) and the new parameter at which the bases are to be interpolated (s).

1. Map to the tangent space using a logarithm map:

$$(I - \Phi_0\Phi_0^T)\Phi_1(\Phi_0^T\Phi_1)^\dagger = U\Sigma V^T$$

$$\Lambda = U\tan^{-1}(\Sigma)V^T.$$

2. Interpolate in the tangent space:

$$\tilde{\alpha} = \frac{s - s_0}{s_1 - s_0}$$

$$\tilde{\Lambda} = U[\tilde{\alpha}\tan^{-1}(\Sigma)]V^T.$$

3. Map back to the Grassman manifold using an exponential map:

$$\Phi(s) = \Phi_0 V\cos\left[\tilde{\alpha}\tan^{-1}(\Sigma)\right] + U\sin\left[\tilde{\alpha}\tan^{-1}(\Sigma)\right].$$

Algorithm 2 General Basis Interpolation

Orthonormal bases $\{\Phi_i\}_{i=0}^n$, associated with parameters, $\{s_i\}_{i=0}^n$

1. Choose a subspace S_0 as a reference and origin point for the interpolation.
2. Each subspace is mapped to a matrix Σ_i representing a point on the tangent space, T_0 using a logarithm map and the SVD:

$$(I - \Phi_0\Phi_0^T)\Phi_i(\Phi_0^T\Phi_i)^\dagger = U_i\Sigma_i V_i^T$$

$$\Gamma_i = U_i\tan^{-1}(\Sigma_i)V_i^T.$$

3. Each entry of the new matrix $\Gamma(s)$ is computed by interpolating the entries of the matrices $\{\Sigma_i\}_{i=1}^n$.
4. The matrix $\Sigma(s)$ is mapped to a subspace on the Grassman manifold spanned by $\Phi(s)$ using an exponential map:

$$\Gamma(s) = U\Sigma V^T$$

$$\Phi(s) = \Phi_0 V\cos(\Sigma) + U\sin(\Sigma).$$

B. Incompressible ROM Formulation

Consider the continuity and Navier-Stokes equations

$$\nabla \cdot u = 0, \tag{1}$$

$$\frac{\partial u}{\partial t} = \frac{1}{Re}\Delta u - \nabla\cdot(uu) - \nabla p. \tag{2}$$

Here $u(x,t)$ is the velocity field of the fluid, Re denotes the Reynolds number, and p is the pressure. The evolution of an incompressible flow is governed by Equations (1) and (2). We consider the Galerkin approximation

$$u(x,t) \approx u_0(x) + \sum_{j=1}^{n} a_j(t)\phi_j(x), \tag{3}$$

where $u_0(x)$ is the arithmetic mean of the provided flow snapshots, $a_i(t)$ are POD coefficients, and $\phi_i(x)$ are the POD modes. We assume $u_0(x)$ satisfies the boundary conditions and $\sum_{j=1}^{n} a_j(t)\phi_j(x)$ quantifies the rest of the flow with homogeneous Dirichlet boundary conditions. A Galerkin projection scheme yields a set of n coupled ODEs

$$M\frac{da}{dt} = a^T Q a + (L^0 + \frac{1}{Re}L^{Re})a + P + C^0 + \frac{1}{Re}C^{Re}, \tag{4}$$

for the modal coefficients [13]. Note that the modal matrices are given by

$$
\begin{aligned}
M_{ij} &= \left(\phi_i(x), \phi_j(x)\right)_\Omega, \\
Q_{ijk} &= -\left(\phi_i, \nabla \cdot (\phi_j \phi_k)\right)_\Omega, \\
L_{ij}^{Re} &= \left(\phi_i, \Delta\phi_j\right)_\Omega, \\
L_{ij}^{0} &= -\left(\phi_i, \nabla \cdot (u_0 \phi_j)\right)_\Omega - \left(\phi_i, \nabla \cdot (\phi_j u_0)\right)_\Omega, \\
C_i^{Re} &= \left(\phi_i, \Delta u_0\right)_\Omega, \\
C_i^{0} &= -\left(\phi_i, \nabla \cdot (u_0 u_0)\right)_\Omega, \\
P_i &= -\left(\phi_i, \nabla p\right)_\Omega,
\end{aligned}
$$

where $(\phi_i, \phi_j)_\Omega = \int_\Omega \phi_i(x)\phi_j(x)d\Omega$ [2]. The mass matrix M reduces to the identity matrix due to the orthonormality of the POD modes. We examine the pressure term,

$$
\begin{aligned}
-\left(\phi_i, \nabla p\right)_\Omega &= -\int_\Omega \phi_i(x)\nabla p d\Omega \\
&= -\int_\Gamma p\phi_i(x) \cdot \hat{n} d\Gamma + \int_\Omega p\nabla \cdot \phi_i(x) d\Omega.
\end{aligned} \tag{5}
$$

Note that the POD modes are linear combinations of the data snapshots, which are divergence-free as illustrated in Equation 1. Therefore, the modes will be divergence free and each mode will satisfy Equation 1. This implies that the second integral in Equation 5 will be zero. Additionally, the modes in the Galerkin decomposition satisfy homogeneous Dirichlet boundary conditions. As such, the surface integral in Equation 5, and consequently the pressure term, will be zero. Then, (4) reduces to

$$
\frac{da}{dt} = a^T Q a + (L^0 + \frac{1}{Re} L^{Re})a + C^0 + \frac{1}{Re} C^{Re}. \tag{6}
$$

The sensitivity of this data set to the numerically nonzero pressure term has been studied previously by the authors [14].

We assess the performance of the parametric reduced-order modeling techniques by testing on 2D regularized lid-driven cavity data [12]. We do so by comparing the kinetic energy and enstrophy time histories to those from the reference data. As the trends presented by the global kinetic energy were qualitatively identical to those presented by the global enstrophy, for brevity only plots of global kinetic energy are presented here.

III. Results and Discussion

Flow data will be sampled from a range of Reynolds numbers at which the lid-driven cavity exhibits a toroidal bifurcation from periodic to chaotic dynamics: Reynolds numbers between 15,000 and 18,000. The dominant frequencies remain coherent but vary with Reynolds number within this range [15]; at higher Reynolds numbers, the flow's frequency spectrum becomes broadband and the dynamics are thus less informative for comparing these different models.

A. Spanning ROM

We form a parametric ROM by first performing POD on a collection of snapshots built from data snapshots corresponding to different parameter values in the parameter space. The collection of snapshots is formed from lid-driven cavity reference data at Reynolds numbers 15,000, 16,000, 17,000, and 18,000. Next, POD is performed to obtain the spanning basis. The spanning basis is then used to construct the ROM matrices and ODE system via Equation (4). The resulting parametric ROM is evaluated over a time period of 6000 time steps (600 s) at the out-of-sample Reynolds numbers Re = 15,500, where the flow changes from periodic to quasiperiodic, Re =16,500, and Re =17,500. We compute the kinetic energy time histories to assess the performance of the parameterized reduced-order model.

The time histories of the kinetic energy for the spanning basis POD-ROM, as well as the results of direct numerical simulation, are shown in Figure 1. The spanning ROM matches the kinetic energy of the direct numerical simulation well at each of the three tested Reynolds numbers. Time histories of global enstrophy were also surveyed and they presented qualitatively identical agreement to these kinetic energy plots.

We observe that the spanning ROM performs well even across bifurcations when the reference data are closely spaced within the parameter space. Next, we increase the separation between the datasets, in terms of the Reynolds number, to

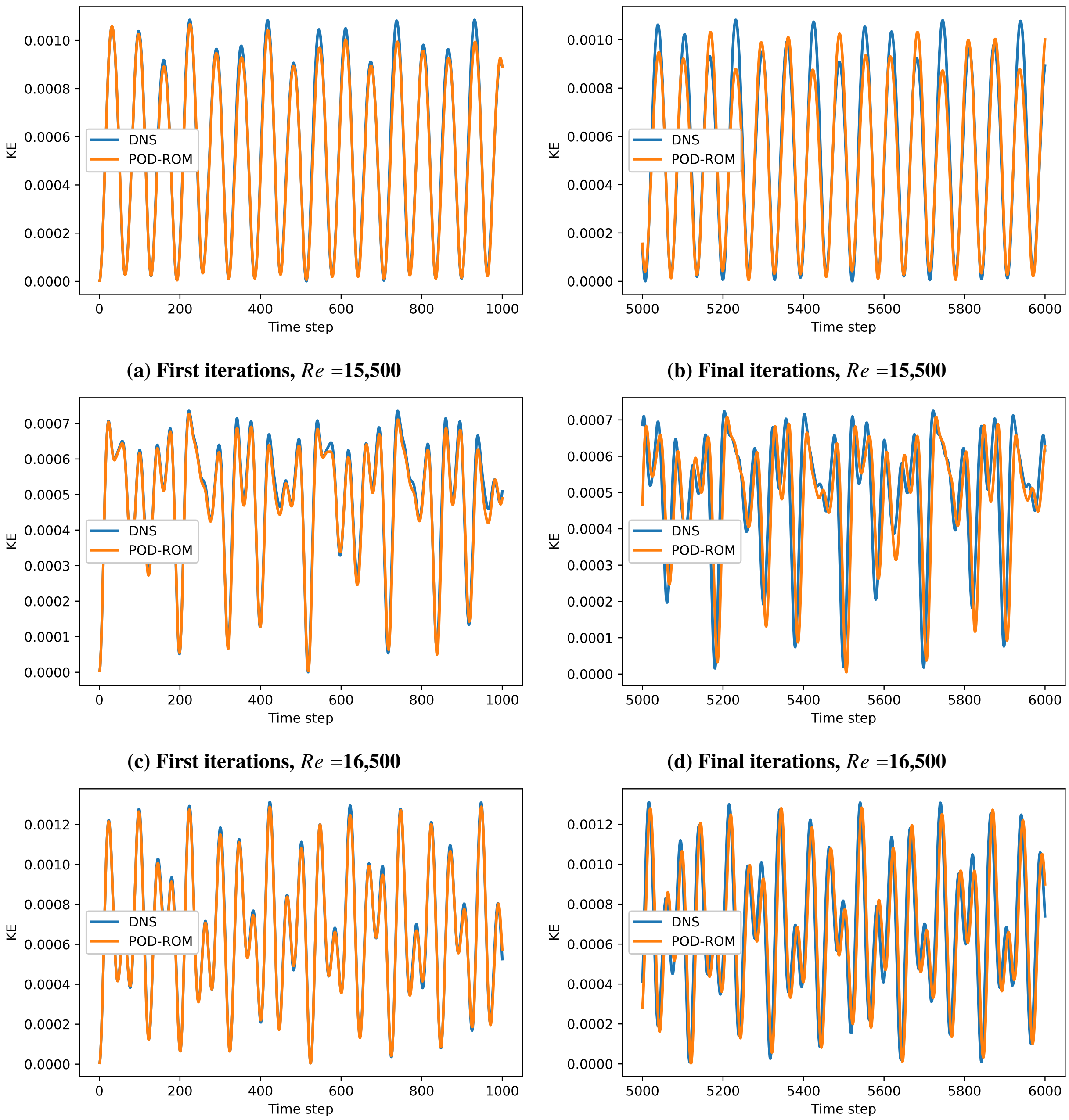

(a) First iterations, Re =15,500

(b) Final iterations, Re =15,500

(c) First iterations, Re =16,500

(d) Final iterations, Re =16,500

(e) First iterations, Re =17,500

(f) Final iterations, Re =17,500

Fig. 1 Comparison of kinetic energy of the spanning ROM [15k|16k|17k|18k] with those of the direct numerical simulation for intermediate Reynolds numbers.

assess how well this parametric ROM approach performs when the datasets aren't as close. We increase the spacing between Reynolds numbers from 1,000 to 1,500, and construct a spanning ROM using data from Reynolds numbers 15,000, 16,500, and 18,000. From Figure 2, we observe that the ROM remains accurate in short-time integration, but loses some stability in long-time integration. The bifurcation at Reynolds number 15,500 is still well-qualified in short-time integration, but stability issues appear after this point. When further increasing the separation between the Reynolds numbers of the training datasets to 2,000, the spanning ROM is still able to retain accuracy in short-time integration, as shown in Figure 3. Here a spanning ROM is constructed using data from Reynolds numbers 14,000, 16,000, and 18,000. The flow at Re =14,000 is periodic, rather than quasi-periodic, so the basis at just this Reynolds number has an order of magnitude fewer modes in it. As such, late-time instabilities are more possible and far more of the basis is defined for higher-Reynolds number flow dynamics.

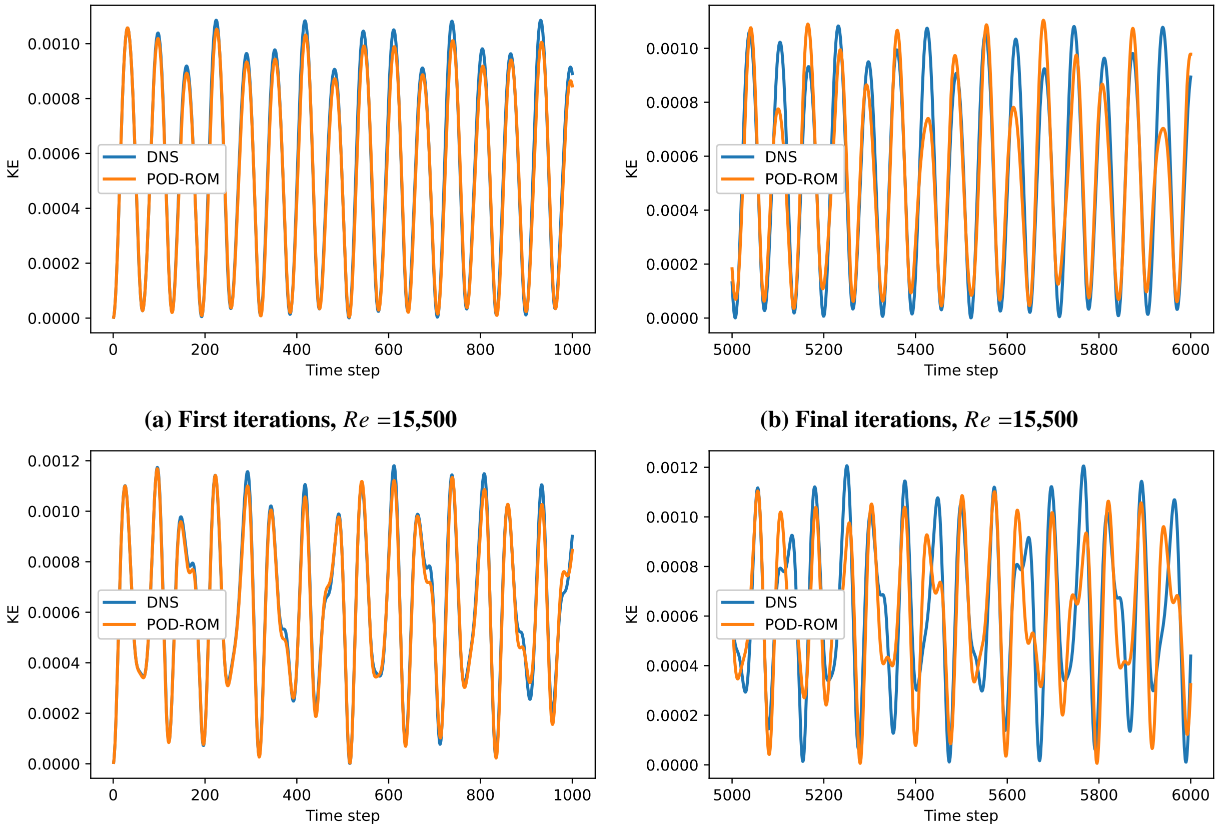

(a) First iterations, Re =15,500

(b) Final iterations, Re =15,500

(c) First iterations, Re =16,000

(d) Final iterations, Re =16,000

Fig. 2 Comparison of kinetic energy of the spanning ROM [15k|16.5k|18k] with those of the direct numerical simulation for intermediate Reynolds numbers.

The disadvantage of the spanning ROM approach is that it requires a large amount of memory to form and store the collection of snapshots, as well as to perform POD on this collection of snapshots. Therefore, this method is not preferable when memory is limited or when the size of the data is excessively large. One can reduce the memory cost of the spanning ROM approach by reducing the number of snapshots and reducing the number of modes in the spanning basis. When taking this approach early in testing, we found the modes of the spanning basis were dominated by the modes from higher Reynolds numbers in the quasiperiodic and aperiodic regimes (for a spanning basis formed from 1,000 snapshots each from datasets Re =14,000 to Re =19,500, excluding Re =17,000, where we wanted to evaluate the resulting ROM). The domination of the larger Reynolds number modes caused the ROM to perform poorly in the quasiperiodic regime.

B. Basis Concatenation

We construct a parametric ROM through concatenation of POD bases computed from reference flow data from different Reynolds numbers. Using data snapshots from regularized lid-driven cavity data [12] at Reynolds numbers 15,000, 16,000, 17,000, and 18,000, a POD basis is constructed for each set of data and concatenated together into a single basis:

$$\Phi_{total} = [\Phi_{15,000}|\Phi_{16,000}|\Phi_{17,000}|\Phi_{18,000}].$$

This concatenated basis is used to form the ROM matrices and ODE system via Equation (4). The resulting parametric ROM is then evaluated at the out-of-sample Reynolds numbers 15,500, 16,500, and 17,500 for 6000 time

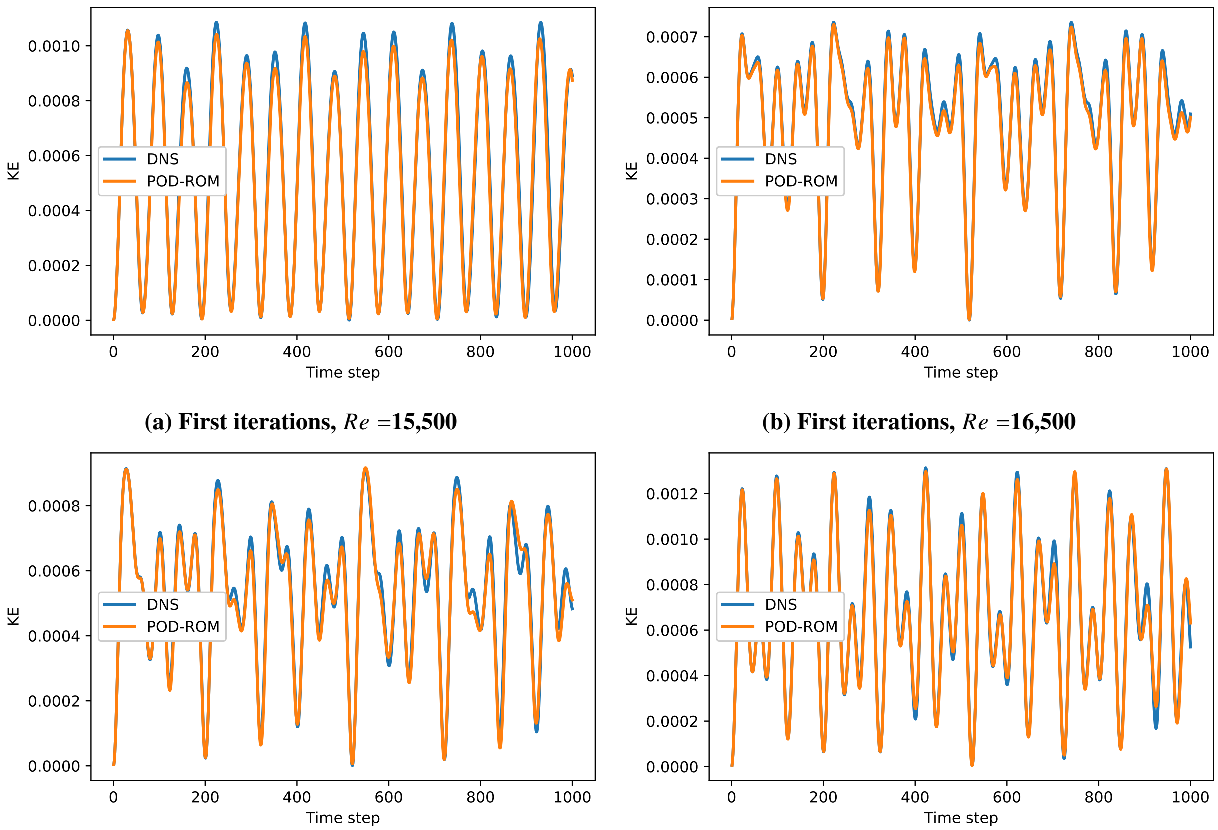

(a) First iterations, *Re* =15,500

(b) First iterations, *Re* =16,500

(c) First iterations, *Re* =17,000

(d) First iterations, *Re* =17,500

Fig. 3 Comparison of kinetic energy of the spanning ROM [14k|16k|18k] with those of the direct numerical simulation for intermediate Reynolds numbers.

steps (600 s). We compute the kinetic energy to assess the performance of the parameterized reduced-order model against direct numerical simulations. We observe in Figure 4 that the kinetic energy of the parametric reduced-order model closely matches that of the direct numerical simulation at each of the three tested Reynolds numbers. We note that the reduced-order flow matches the dominant frequencies of the reference data over the entire 6000 time step simulation. With this relatively close separation between the Reynolds numbers, we note that the bifurcation at Reynolds number 15,500 is well qualified as the flow becomes quasiperiodic, as seen in Figure 4.

As with the spanning ROM, we increase the separation between the datasets used to construct the basis concatenation ROM and observe the effect on the reduced-order model. A basis concatenation ROM is constructed from POD bases corresponding to Reynolds numbers of 15,000, 16,500, and 18,000 to test the effect of increasing the separation between the Reynolds numbers of the reference datasets. When the separation between the POD bases used to form the concatenate basis is increased to 1,500 between each Reynolds number, we observe that the reduced-order model retains accuracy in short-time integration, but performs worse in longer time integration for some Reynolds numbers, as shown in Figure 5. With this additional separation between the Reynolds numbers of the POD bases, we observe that the bifurcation at Reynolds number 15,500 is still well modeled in short-time integration, but is not so when looking at longer time integration.

Similarly, if the separation between Reynolds numbers is increased to 2,000, ROM performance becomes more inconsistent, with some choices of training datasets performing better than others at certain Reynolds numbers. For example, a ROM formed using a concatenated basis from Reynolds numbers 14,000, 16,000, and 18,000 outperforms one built using a concatenated basis from Reynolds numbers 15,000, 17,000, and 19,000 at Reynolds number 17,500 as shown in Figure 6.

The basis concatenation method has the disadvantage that the basis can quickly grow large as more bases are concatenated together, especially when these bases have many modes. Therefore, this method is less suited for the range

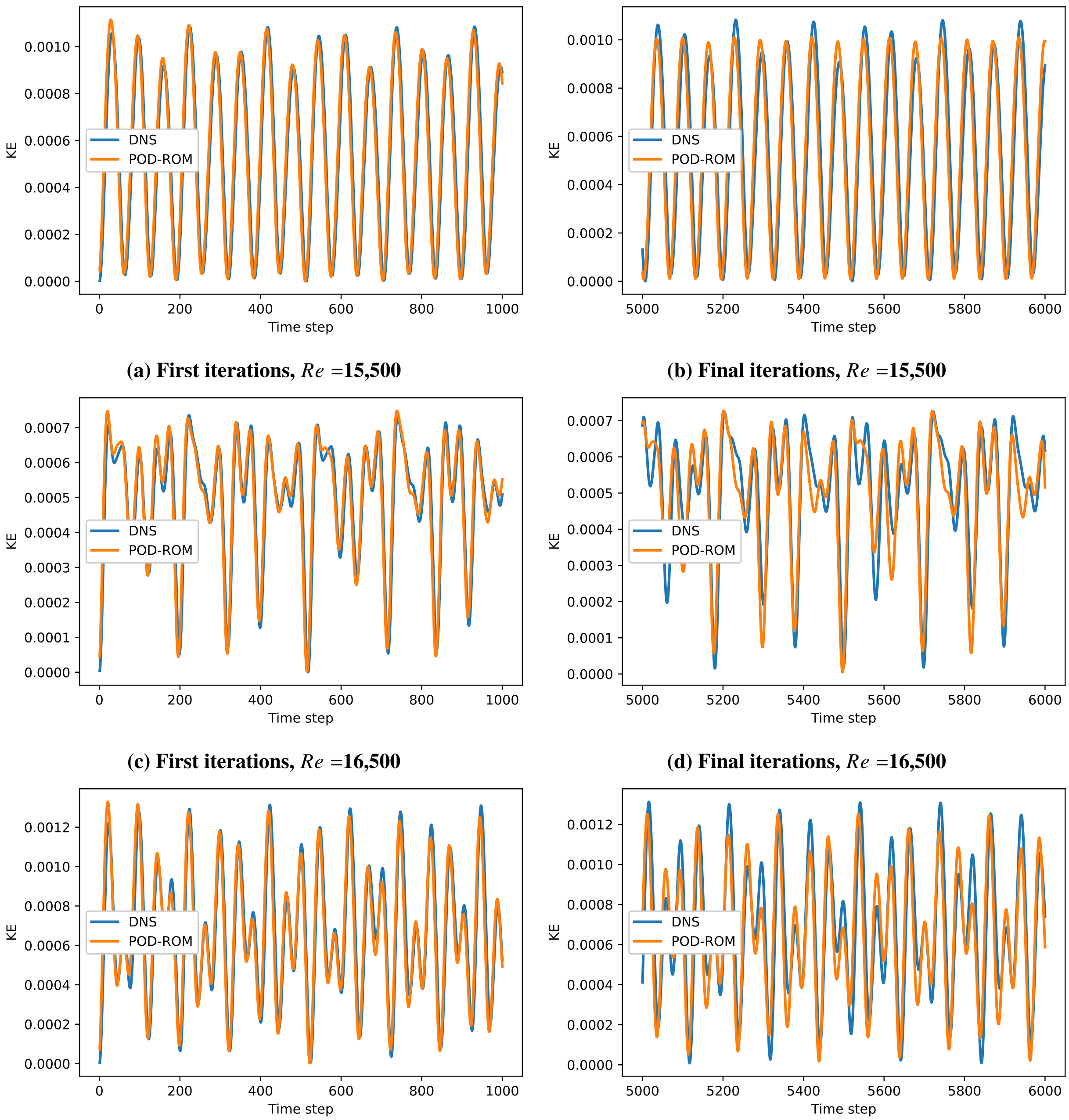

(a) First iterations, Re =15,500

(b) Final iterations, Re =15,500

(c) First iterations, Re =16,500

(d) Final iterations, Re =16,500

(e) First iterations, Re =17,500

(f) Final iterations, Re =17,500

Fig. 4 Comparison of kinetic energy of the basis concatenation ROM [15k|16k|17k|18k] with those of the direct numerical simulation for intermediate Reynolds numbers. The first 450 modes were retained in the single basis that yielded all of these results.

of turbulent Reynolds numbers, which requires a large number of modes to retain a significant portion of the kinetic energy. As the number of modes in the basis increases, the matrix Q among the ROM matrices becomes exceedingly computationally expensive to compute and store. Basis concatenation parametric ROMs are also more susceptible to numerical noise than the spanning ROM since it contains more higher order modes, which are affected by numerical noise when the resolution of the data is low. To address these weaknesses, rank-deficient components may be removed by a singular value decomposition or rank-revealing QR factorization to decrease the size and obtain an orthonormal basis [5]. This was not performed in the present work.

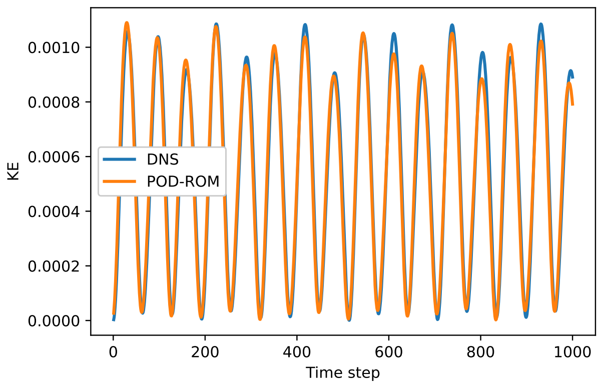

(a) First iterations, Re =15,500

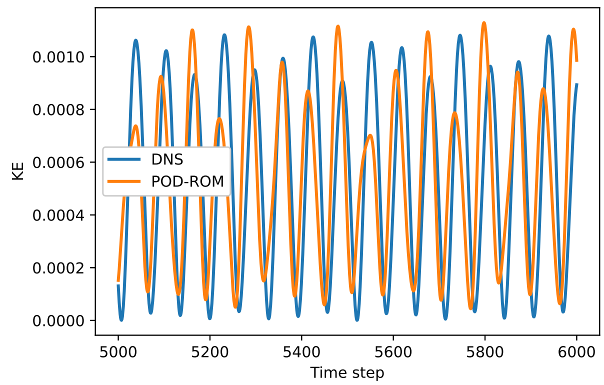

(b) Final iterations, Re =15,500

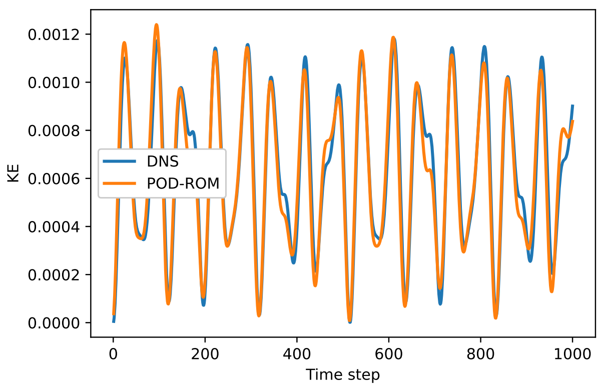

(c) First iterations, Re =16,000

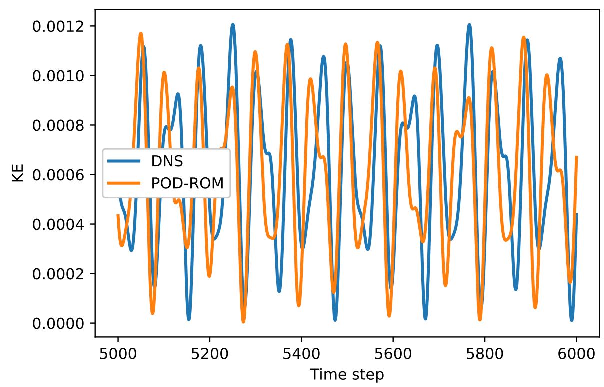

(d) Final iterations, Re =16,000

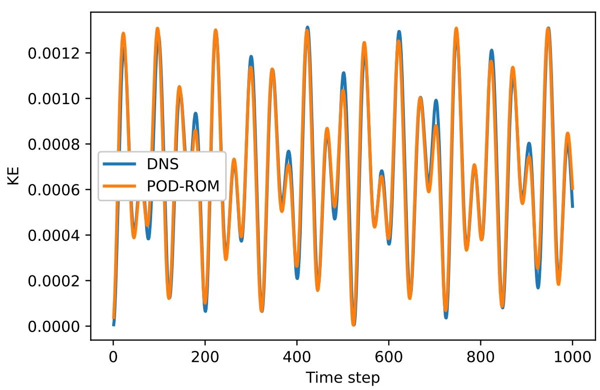

(e) First iterations, Re =17,500

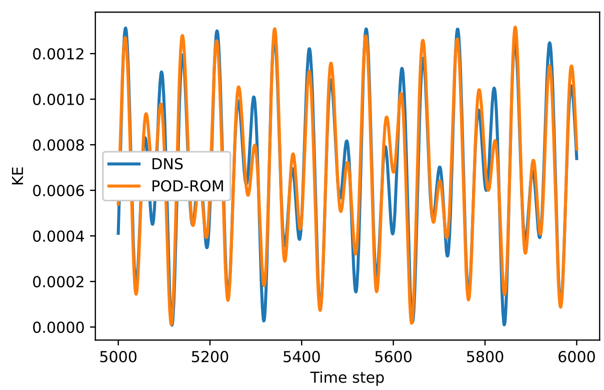

(f) Final iterations, Re =17,500

Fig. 5 Comparison of kinetic energy of the basis concatenation ROM [15k|16.5k|18k] with those of the direct numerical simulation for intermediate Reynolds numbers. The first 340 modes were retained in the single basis that yielded all of these results.

This approach is very well suited to incompressible flows requiring few modes. Once the incompressible ROM matrices have been computed for a particular basis, the matrices do not need to be recomputed to adapt the ROM for a new Reynolds number; only the Reynolds number in the formulation needs to be adjusted. This makes the basis concatenation ROM very computationally efficient when the concatenated basis contains less than a few hundred modes, permitting this method to be used for uncertainty quantification using MCMC methods. If the ROM matrices are dependent on the parameters, the ROM matrices have to be recomputed to evaluate the ROM at a new Reynolds number. To maintain computational efficiency, one may employ the strategy of Ref. [6] and utilize interpolation of ROM matrices

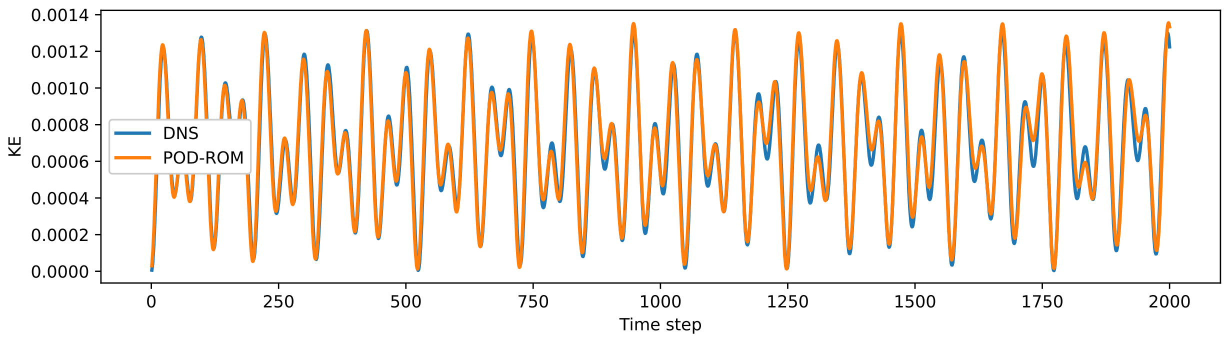

(a) First iterations, [14k|16k|18k] parametric ROM

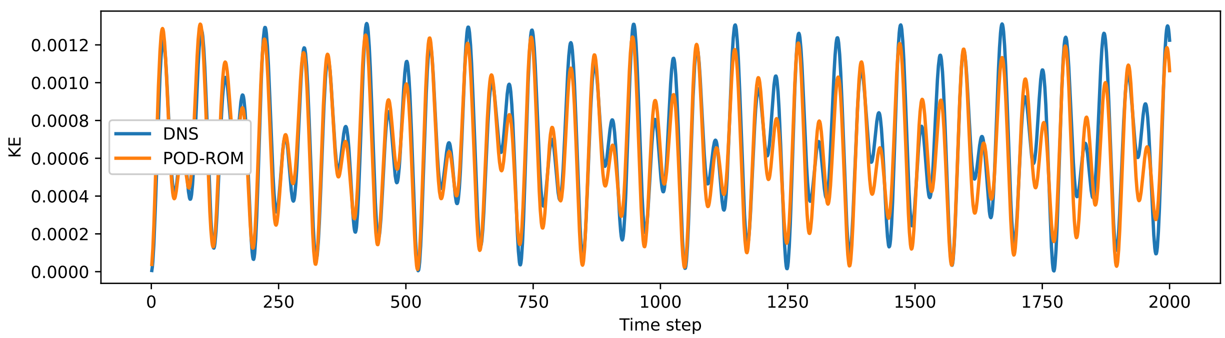

(b) First iterations, [15k|17k|19k] parametric ROM

Fig. 6 Comparison of the kinetic energy time histories of the parametric ROMs built from concatenated bases [14k|16k|18k] and [15k|17k|19k] at Reynolds number Re=17,500, respectively.

to efficiently compute the ROM matrices for new parameter values.

C. Basis Interpolation

The final method we investigate is the basis interpolation approach to constructing parametric reduced-order models. In this approach, a parametric ROM is constructed by interpolating POD bases corresponding to separate Reynolds numbers as outlined in Algorithm 1. We interpolate the POD bases computed from regularized lid-driven cavity data [12] at Reynolds numbers 16,000 and 17,500, with the origin for the transformation to the tangent space being Reynolds number 16,500. From Figure 7, we see that the kinetic energy of the general basis interpolation parametric ROM matches that of the direct numerical simulation. What is more, we note that the general basis interpolation formula produces a more stable ROM than the one obtained from the univariate basis interpolation algorithm.

This shortcoming of the univariate basis interpolation procedure is not always apparent, however. In Figure 8, we observe two univariate basis interpolation ROMs with different target Reynolds numbers but the same interval between target and source Reynolds numbers. Despite the similarity in setup, the particular Reynolds numbers of interest yielded better results in one case than the other. The relative number of modes in each source basis seems to inform this shortcoming: the more disparate, the less accurate the interpolated ROM is likely to be.

In terms of utility, basis interpolation is useful when there are parameters of interest that are not explicitly in the ROM formulation. The downside of basis interpolation is that the ROM matrices must be recomputed to adjust the ROM to new parameter values. Computationally, this makes basis interpolation less appealing for the incompressible ROM formulation in comparison to the spanning ROM and basis concatenation approaches. However, basis interpolation is useful when the spanning ROM and basis concatenation techniques may be too memory intensive or use an excessive amount of modes that cause the ROM to be computationally inefficient. The general basis interpolation ROM is expected to more useful when considering multiple parameters, especially when data are available at many parameter values in the parameter space.

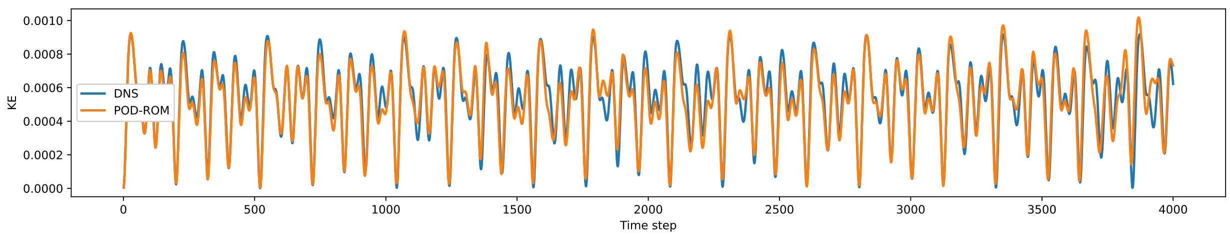

(a) General basis interpolation, first iterations

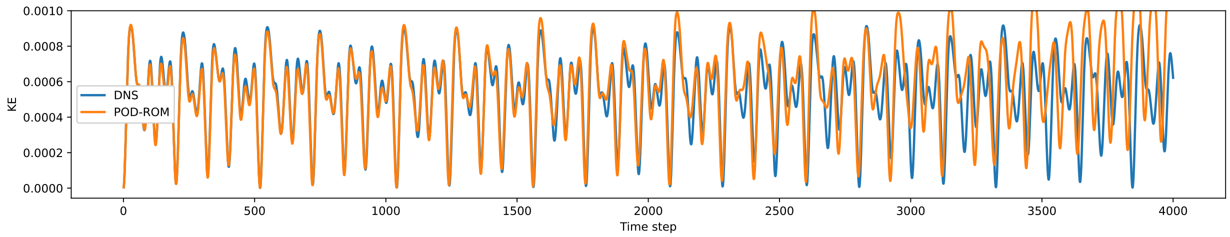

(b) Univariate basis interpolation, first iterations

Fig. 7 Comparison of kinetic energy of the general basis interpolation ROM [16k|17.5k] (top) and the univariate basis interpolation ROM [16.5k|17.5k] (bottom) for new Reynolds number 17,000.

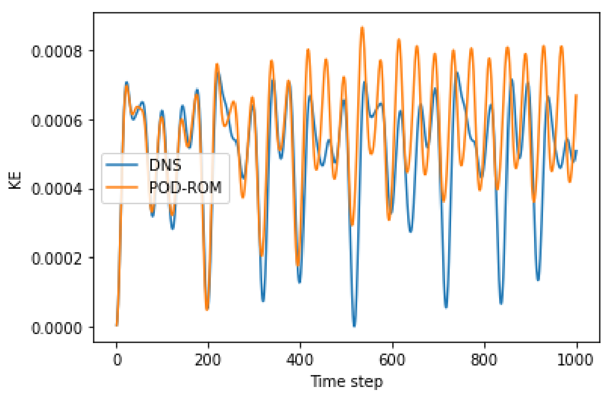

(a) [15.5k|17.5k] Univariate Basis Interp., *Re* =16,500

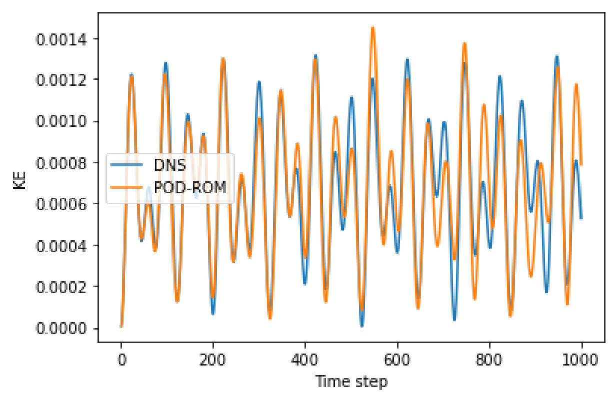

(b) [16.5k|18.5k] Univariate Basis Interp., *Re* =17,500

Fig. 8 Comparison of kinetic energy for two univariate basis interpolation ROMs with a separation in Reynolds number of 2,000.

D. Conclusions

We have investigated three different techniques to produce fluid reduced-order models at conditions not directly studied by higher fidelity tools. All three methods presented different strengths and weaknesses when applied to the same source data, indicating that each has utility in different kinds of applications.

The spanning and basis concatenation parametric ROMs yielded very similar results. It was shown that these two approaches yield parametric ROMs capable of accurate fluid flow simulations even in long-time integration when the Reynolds numbers used to construct them are relatively close. When the separation of the Reynolds numbers of the reference data or POD bases used to construct the parametric ROMs was increased, it was shown that these parametric ROMs preserve accuracy in short-time integration, but stability in long-time integration is less consistent. The primary difference between these techniques lies in the resources required to construct the ROMs in the first place: the spanning ROM requires a large amount of memory to load the snapshots from all reference data points and perform the single basis construction step, whereas the concatenation ROM does not require this large up-front memory requirement but does require the ROM itself to include more modes to perform well, as the basis size grows with the number of parameter points included in the source data.

Basis interpolation proved less robust than the spanning and basis concatenation parametric ROM techniques for the incompressible formulation. The univariate basis interpolation ROMs were only accurate for short-time integration using bases close to the Reynolds number of interest. The general basis interpolation vastly improved the stability of the basis interpolation ROMs, but did not reach the performance of the spanning and basis concatenation ROMs. However, this technique allows for both small snapshot sets and small basis sizes, and thus for smaller interpolation distances this technique is preferable to the other two. The general basis interpolation ROM is also expected to prove more useful when considering multiple parameters or parameters not explicitly included in the governing equations and boundary conditions due to the explicit nature of the interpolation algorithm.

With this methodological study complete on a well-known test problem, work is now ongoing to test these parametric ROMs as a part of aerodynamic database generation for application to EDL applications. These ROMs will provide one data source for the data fusion techniques compiled as a part of the AeroFusion initiative [1].

Acknowledgments

This work was authored by employees of North Carolina State University under Contract No. 80LARC21CA003 and the University of Southern California under Contract No. 80LARC21CA002 with the National Aeronautics and Space Administration. The United States Government retains and the publisher, by accepting the article for publication, acknowledges that the United States Government retains a nonexclusive, paid-up, irrevocable, worldwide license to reproduce, prepare derivative works, distribute copies to the public, and perform publicly and display publicly, or allow others to do so, for United States Government purposes. All other rights are reserved by the copyright owner.

References

[1] Snyder, S., Wignall, T., Green, J. S., Kumar, S. G., Lee, M. W., Nakamura-Zimmerer, T., Scoggins, J. B., and Williams, R. A., "AeroFusion: Data Fusion and Uncertainty Quantification for Lander Vehicles," *AIAA Science and Technology Forum and Exposition*, 2023, submitted.

[2] Balajewicz, M. J., Dowell, E. H., and Noack, B. R., "Low-dimensional modelling of high-Reynolds-number shear flows incorporating constraints from the Navier–Stokes equation," *Journal of Fluid Mechanics*, Vol. 729, 2013, pp. 285–308.

[3] Weller, J., Lombardi, E., Bergmann, M., and Iollo, A., "Numerical methods for low-order modeling of fluid flows based on POD," *International Journal For Numerical Methods in Fluids*, Vol. 63, 2010, pp. 249–268.

[4] Taira, K., Brunton, S. L., Dawson, S. T., Rowley, C. W., Colonius, T., McKeon, B. J., Schmidt, O. T., Gordeyev, S., Theofilis, V., and Ukeiley, L. S., "Modal analysis of fluid flows: An overview," *Aiaa Journal*, Vol. 55, No. 12, 2017, pp. 4013–4041.

[5] Benner, P., Gugercin, S., and Willcox, K., "A survey of projection-based model reduction methods for parametric dynamical systems," *SIAM review*, Vol. 57, No. 4, 2015, pp. 483–531.

[6] Degroote, J., Vierendeels, J., and Willcox, K., "Interpolation among reduced-order matrices to obtain parameterized models for design, optimization and probabilistic analysis," *International Journal for Numerical Methods in Fluids*, Vol. 63, No. 2, 2010, pp. 207–230.

[7] Amsallem, D., and Farhat, C., "Interpolation method for adapting reduced-order models and application to aeroelasticity," *AIAA journal*, Vol. 46, No. 7, 2008, pp. 1803–1813.

[8] Bui-Thanh, T., Willcox, K., and Ghattas, O., "Parametric reduced-order models for probabilistic analysis of unsteady aerodynamic applications," *AIAA journal*, Vol. 46, No. 10, 2008, pp. 2520–2529.

[9] Choi, Y., Boncoraglio, G., Anderson, S., Amsallem, D., and Farhat, C., "Gradient-based constrained optimization using a database of linear reduced-order models," *Journal of Computational Physics*, Vol. 423, 2020, p. 109787.

[10] Deng, N., Noack, B. R., Morzyński, M., and Pastur, L. R., "Low-order model for successive bifurcations of the fluidic pinball," *Journal of fluid mechanics*, Vol. 884, 2020.

[11] Sternfels, R., and Earls, C., "Reduced-order model tracking and interpolation to solve PDE-based Bayesian inverse problems," *Inverse Problems*, Vol. 29, 2013.

[12] Lee, M. W., "Steady State 2D Regularized Lid-Driven Cavity Low-resolution Spatiotemporal Snapshots - Part 3 of 3," =https://data.mendeley.com/datasets/74g8rjfkvt/1, 2021. https://doi.org/10.17632/74g8rjfkvt.1.

[13] Lee, M. W., "On Improving the Predictable Accuracy of Reduced-order Models for Fluid Flows," Ph.D. thesis, Duke University, 2020.

[14] Lee, M. W., and Dowell, E. H., "On the Importance of Numerical Error in Constructing POD-based Reduced-Order Models of Nonlinear Fluid Flows," *AIAA Scitech 2020 Forum*, 2020, p. 1067.

[15] Lee, M. W., Dowell, E. H., and Balajewicz, M. J., "A study of the regularized lid-driven cavity's progression to chaos," *Communications in Nonlinear Science and Numerical Simulation*, Vol. 71, 2019, pp. 50–72.